ISSN 1075-7015, Geology of Ore Deposits, 2006, Vol. 48, No. 4, pp. 326–334. © Pleiades Publishing, Inc., 2006.
Original Russian Text © A.I. Gorshkov, S.V. Titkov, Yan Nan Bao, I.D. Ryabchikov, L.O. Magazina, 2006, published in Geologiya Rudnykh Mestorozhdenii, 2006, Vol. 48, No. 4, pp. 375–384.

Microinclusions in Diamonds of Octahedral Habit from Kimberlites of Shandong Province, Eastern China

A. I. Gorshkov[a]*, S. V. Titkov[a], Yan Nan Bao[b], I. D. Ryabchikov[a], and L. O. Magazina[a]

[a] *Institute of Geology of Ore Deposits, Petrography, Mineralogy, and Geochemistry, Russian Academy of Sciences, Staromonetnyi per. 35, Moscow, 119017 Russia*

[b] *Mining University of China, Xiyuan 11, Beijing, 100083 China*

Received July 20, 2005

Abstract—Microinclusions in octahedral diamond crystals from kimberlites of Shandong Province, eastern China, have been studied with analytical scanning electron microscopy. Native iron, tungsten, and lead; Fe–Cr intermetallic compounds; polydymite; ilmenite; halite; and matlockite (PbFCl) have been identified on the crystal surfaces. Microinclusions of native iron and chrome, Fe–Cr intermetallic compounds, pentlandite, Cr-free garnet, calcite, and apatite, as well as a relatively large (100×270 μm) inclusion representing an intergrowth of clinopyroxene, calcite, and apatite, have been revealed on the surfaces of fresh chips of the samples. The deep geological processes that could have resulted in the formation of such unusual mineral assemblages are discussed in the light of new experimental data.

DOI: 10.1134/S1075701506040064

INTRODUCTION

Since intense investigations of mineral inclusions in diamonds from kimberlites started in China only in the mid-1980s, these inclusions have until now remained poorly studied as compared with inclusions in diamonds from the well-known African and Yakutian deposits. Relatively large inclusions distinguishable under an optical microscope were studied in representative collections (tens of thousands of samples) of diamonds from Liaoning (Harris et al., 1994; Meyer et al., 1994) and Shandong (Meyer et al., 1994) provinces. It was established that mineral inclusions of the ultramafic assemblage (olivine, chromite, enstatite, Cr-garnet, sulfides) are predominant. Minerals of the eclogite assemblage (garnet, omphacite) were revealed more rarely.

The study of microinclusions in diamonds from the China kimberlites by analytical scanning electron microscopy showed their great variety. Native iron and chrome, Fe–Cr–Ni and Bi–Te–Sb intermetallic compounds, Cr-spinel, magnetite, rutile, chalcopyrite, apatite, graphite, calcite, and some other minerals were detected in almost opaque diamonds of cubic habit from Liaoning Province (Vinokurov et al., 1998; Gorshkov et al., 1997a). Microinclusions of olivine, native iron and lead, Fe–Cr solid solutions, sulfides (gersdorffite, siegenite, and polydymite), apatite, phlogopite, and other minerals were established in polycrystalline aggregates of octahedral diamond microcrystals from kimberlites of Shandong Province (Gorshkov et al., 1999, 2000). Along with inclusions of native iron, sporadic inclusions of native silver and Fe–Au intermetallic compounds with a Ag admixture were also revealed in diamonds from the China deposits (Zhao, 1995).

Microingrowths of lonsdaleite phase with hexagonal packing of carbon, as well as many inclusions of sellaite and fluorite along with other minerals (zircon, magnetite, rutile, graphite, siderite, and barite), were detected in some diamond microcrystals (Gorshkov et al., 1997b).

Microingrowths of silicon carbide (polytypes 6H and 3C) surrounded by a thin layer of K–Al–Si glass with carbonate and calcium sulfate microsegregations were also established in diamonds from the China deposits (Leund, 1990).

The purpose of this work was to study mineral microinclusions in octahedral diamond crystals from kimberlites of Shandong Province in eastern China using analytical scanning electron microscopy.

As elsewhere, crystals of octahedral habit and rhombic dodecahedrons formed as products of their dissolution are the most abundant morphological type of diamonds in kimberlites of Shandong Province.

The studied transparent crystals were about 2 mm across and contained a small amount of black inclusions. Crystals 1–3 were taken from the Shengli kimberlite pipe and crystal 4, from the Hongxi kimberlite pipe.

RESEARCH METHODS

Microinclusions in diamond crystals from kimberlite pipes of eastern China were studied on a JSM5-5300 scanning electron microscope (Japan) equipped with a

*Address for correspondence: A.I. Gorshkov. E-mail: gai@igem.ru

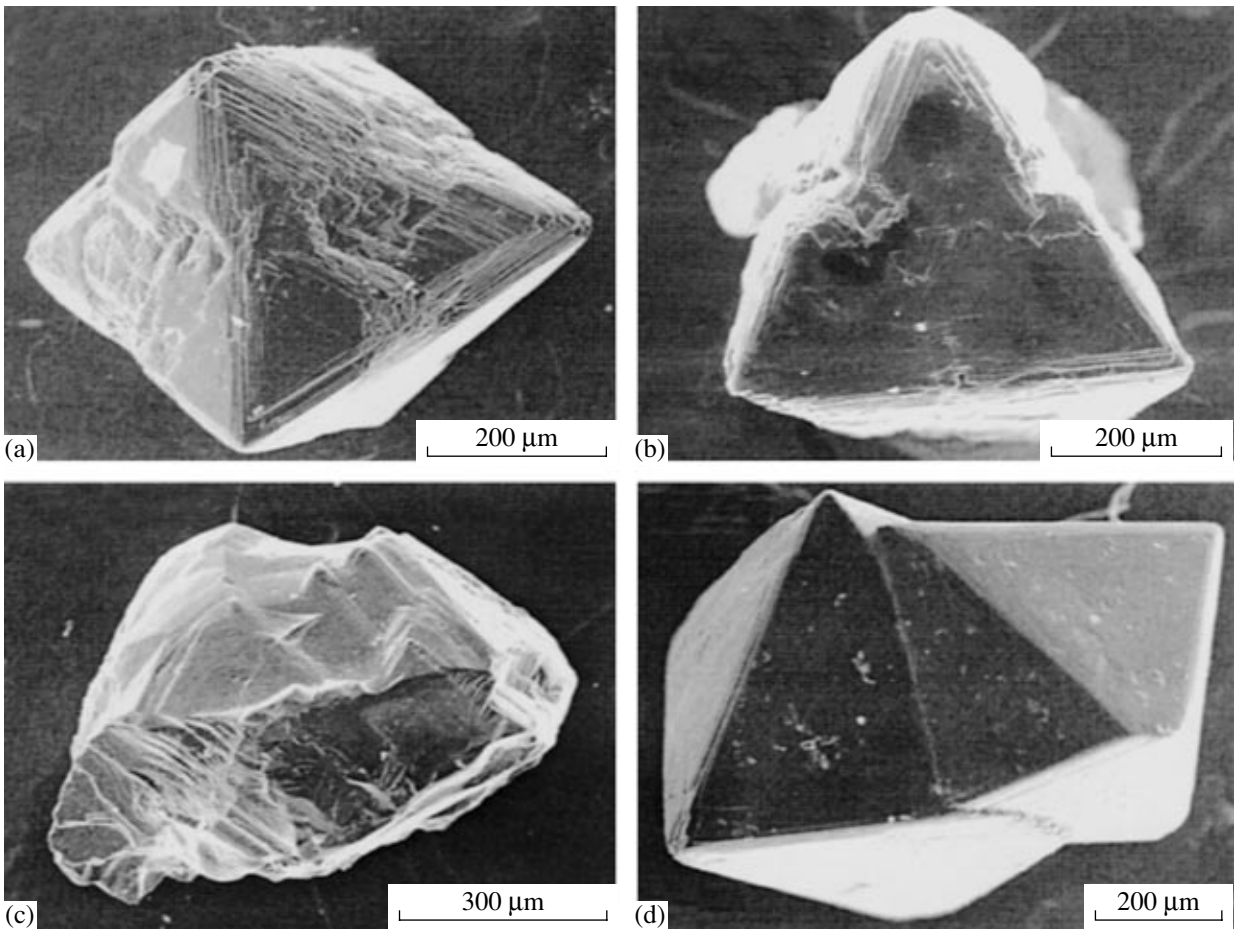

Fig. 1. Morphology of diamond crystals. SEM images in secondary electrons. (a) Sample 1; (b) sample 2; (c) sample 3; (d) sample 4.

Link ISIS energy dispersive spectrometer (United Kingdom), which allows detection of chemical elements from Be to U (oxygen included) in particles fractions of a micron in size.

First, the morphology of diamonds was studied along with microinclusions on their surface. Then the diamonds were split on a diminutive metallic anvil, taking precautions to avoid the contamination of specimens by metallic particles. For this purpose, a diamond sample was wrapped in several layers of heavyweight paper. Afterwards, microinclusions from inner parts of diamonds were studied on fresh surfaces of split chips. Prior to the study, thin carbon films were sprayed on diamonds and their chips for charge sinking. The chemical composition of microinclusions was analyzed on unpolished surfaces, so the results should be considered semiquantitative. Nevertheless, their accuracy was quite sufficient for identification of mineral phases.

MORPHOLOGY OF DIAMOND CRYSTALS

Sample 1 is a distorted diamond crystal of octahedral habit with thin parallel–jagged striation (Fig. 1a). Typical etching trigons are observed on its surface. It also has a sizable mechanical fracture, probably, of technogenic origin, on one side.

Sample 2 is a crystal of octahedral habit with jagged striation and polycentric development of crystal faces (Fig. 1b). A considerable mechanical fracture, probably of technogenic origin, is observed on one side.

Sample 3 is a chip of a highly distorted crystal of octahedral habit with polycentric development of crystal faces (Fig. 1c). It has uneven, rounded surfaces with a blocky sculpture as a result of postcrystallization dissolution. One of its apexes was chopped off and a rather large inclusion was exposed, as is clearly seen in the BSE image.

Sample 4 is an irregular intergrowth of two octahedrons with almost flat faces and insignificant parallel striation on crystal edges (Fig. 1d). Separate etching trigons are developed on faces.

MICROINCLUSIONS EXPOSED ON DIAMOND CRYSTAL SURFACES

Mineral particles and their aggregates and segregations exposed on the surface of octahedral diamond

crystals usually occur at growth steps; in microfractures or caverns; or, less frequently, on relatively even faces.

Crystal 1

Fe–Cr intermetallic compounds are the main minerals found on the surface of this crystal. The prevalence of Fe over Cr and compositional similarity are their distinctive features. Intermetallic compounds of the compositions $Fe_{87}Cr_{13}$, $Fe_{85}Cr_{15}$, and $Fe_{80}Cr_{20}$ were identified from the results of the semiquantitative analysis. These compounds occur as separate micron-sized particles and their aggregates. They are mainly confined to growth steps of the crystal. The energy dispersive (ED) spectra obtained for these intermetallic compounds yielded only Fe and Cr peaks.

In addition, some other mineral phases were detected on the crystal surface in minor amounts.

Native tungsten. Several particles of this metal were detected. One of them, ~2.5 μm in size, occurs in a small hollow formed during the diamond crystal growth (Fig. 2a). The ED spectrum yielded only W peaks (Fig. 2b). Small carbon peaks, here and hereafter, belong to diamond.

Native lead. Discrete isometric particles of this metal tenths of a micron in size occur on a relatively smooth surface of the diamond crystal faces (Fig. 2c). The ED spectra contain only Pb peaks (Fig. 2d).

Quenselite ($PbMnO_2OH_3$). Separate particles and aggregates of the mineral are commonly arranged along growth steps of the diamond crystal. They vary in size from fractions of a micron to several microns; the aggregates reach 20 μm in size. The ED spectrum obtained for one of the aggregates yielded mainly O, Pb, and Mn peaks, as well as small peaks of Ca and Ti impurities. According to the results of the semiquantitative analysis, the Pb : Mn ratio equals 1 : 1, as is typical of quenselite.

Crystal 2

Fe–Cr intermetallic compounds are predominant on the surface of this crystal but occur in a smaller amount as compared with diamond crystal 1. Fe–Cr intermetallic compounds are represented by elongated aggregates arranged along growth steps of the diamond crystal and by isometric and occasionally rectangular particles 1–5 μm in size. As was detected by the semiquantitative analysis, Fe prevails over Cr. The Fe : Cr ratio is close to that in the intermetallic compounds of crystal 1. Furthermore, a Fe–Cr intermetallic compound $Cr_{73}Fe_{27}$ was revealed.

Several other mineral phases were identified in this diamond in lesser amounts.

Native iron. This mineral was found in microfractures on an uneven surface of the diamond crystal as clusters of micron-sized particles. The ED spectra yielded Fe peaks only.

Matlockite (PbFCl). One elongated particle of this mineral was revealed on a crystal surface exhibiting a stepped relief. The particle is 15 μm long and 2.5–0.6 μm wide. As follows from the ED spectrum, the mineral consists of Pb, Cl, and F; Al, Mn, and Fe were detected in minor amounts. The semiquantitative analysis yielded Pb : F : Cl = 1 : 1 : 1, as is typical of matlockite.

Crystal 3

Fe–Cr intermetallic compounds are also prevalent in this crystal. Both discrete particles from one to several microns in size and aggregates of a size exceeding 10 μm were revealed. The ED spectra show only Fe and Cr peaks. As was established by the semiquantitative analysis, Fe always prevails over Cr and the Fe : Cr ratio is nearly equal to this ratio in the corresponding inclusions from diamond crystals 1 and 2.

Native iron. This mineral was established on the surface of diamond crystal 3 as micron-sized separate particles and their chains confined to growth steps of the crystal. The ED spectra exhibit only Fe peaks.

Polydymite (Ni_3S_4). Several oval particles of this mineral were found on a relatively even surface of the crystal face (Fig. 2e). The size of particles is 1 μm. The ED spectra (Fig. 2f) exhibit only Ni and S peaks. The peaks of some impurities from silicate particles occurring nearby were also recorded. An Ni : S ratio of 3 : 4 was established by the semiquantitative analysis. This allowed this mineral to be referred to polydymite.

Crystal 4

Fe–Cr intermetallic compounds are observed as separate isometric particles and as aggregates and clusters. They are exposed on the even surface of crystal faces and are confined to growth steps of the crystal. Iron in these compounds always prevails over chrome. The compositions $Fe_{82}Cr_{18}$, $Fe_{86}Cr_{14}$, and $Fe_{87}Cr_{13}$ were established by the semiquantitative analysis.

Native iron particles were occasionally found on the surface of this crystal. The largest particles are as long as 5 μm. The ED spectra always exhibit a small silicon peak.

Amphibole. Two linearly arranged phases were revealed along the boundary of the two octahedral diamond microcrystals grown together. One of these phases contains Na, Mg, Si, Fe, K, and Ca in proportions characteristic of silicates from the amphibole group.

Mn-bearing ilmenite. This mineral was detected in close association with amphibole and differs from it by a higher brightness. Judging from the spatial relationship between these two phases, amphibole was crystallized earlier than ilmenite. The ED spectrum for one of the sectors of this aggregate exhibits Ti, Fe, Mn, and O peaks. The formula of this mineral was calculated as

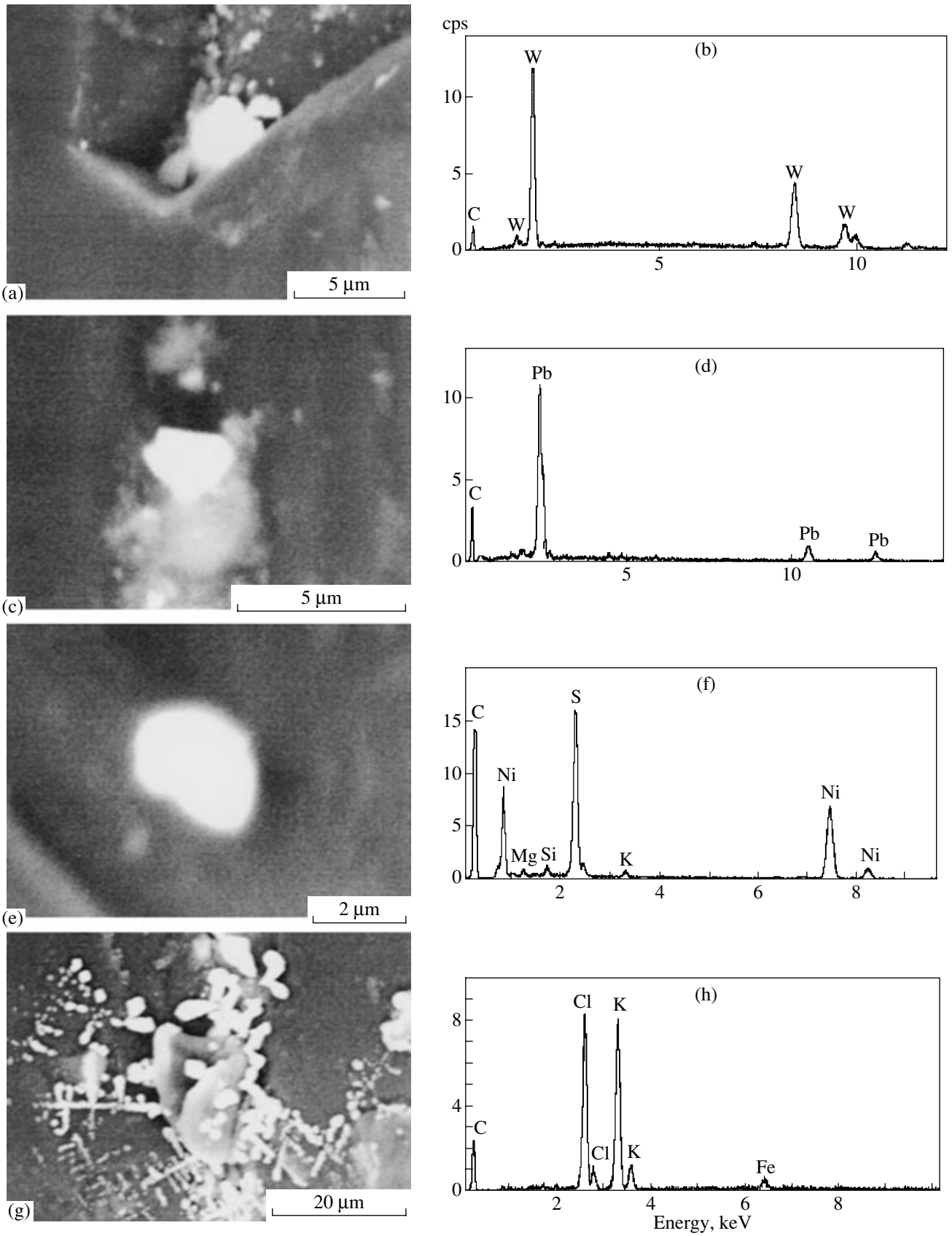

Fig. 2. BSE images and ED spectra of microinclusions exposed on the surface of diamond crystals. (a, b) Native tungsten; (c, d) native lead; (e, f) polydymite; (g, h) sylvite.

$(Mn_{0.18}Fe_{0.82})TiO_3$ from the result of the semiquantitative analysis. According to this formula, the mineral belongs to the ilmenite subgroup (Semenov, 1998) and has a composition transitional between ilmenite ($FeTiO_3$) and pyrophanite ($MnTiO_3$) but is closer to ilmenite. Therefore, this mineral may be called Mn-bearing ilmenite.

Sylvite (KCl). Segregations of this mineral were revealed on the even surface of one of the crystal faces. The segregations are dendritic and consist of isometric and elongated crystals varying from fractions of a micron to several microns in size (Fig. 2g). Smaller crystals make up networks. The ED spectra, one of which is shown in Fig. 2h, demonstrate K and Cl peaks. Insignificant Fe and Cu peaks are related to mechanical impurities. According to the semiquantitative analysis, the K : Cl ratio equals 1 : 1. An insignificant Fe peak indicates a mechanical impurity.

INCLUSIONS THAT OCCUR WITHIN OCTAHEDRAL DIAMONDS

Crystal 1

Native iron (α-Fe). Several particles and native iron aggregates as large as 0.2–0.3 μm were revealed. The ED spectra include the main Fe peaks and insignificant Mn and Co peaks. According to the semiquantitative analysis, the Mn content is 1.5 wt % and the Co content is about 1 wt %.

Fe–Cr intermetallic compounds occur as numerous particles and aggregates. In particular, a feather-shaped aggregate 20 μm in size was found (Fig. 3a). The ED spectra of intermetallic compounds yield Fe and Cr peaks; Fe always prevails over Cr (Fig. 3b). According to the semiquantitative analysis, the Cr content in intermetallic compounds varies from 0.8 to 11 wt %.

Calcite ($CaCO_3$). Several isometric calcite aggregates as large as 5–7 μm were found. Their ED spectra are characterized by Ca, C, and O peaks. According to the semiquantitative analysis, these elements occur in the ratio 1 : 1 : 3, which allowed us to write the formula as $CaCO_3$.

Crystal 2

Native chrome. This metal is represented in the diamond by a rather large isometric aggregate about 10 μm in size (Fig. 3c). The aggregate is surrounded by a scattering of nanoparticles of this metal. The ED spectrum of the aggregate includes the main Cr peaks and an insignificant Ca peak characterizing a mechanical impurity (Fig. 3d).

Fe–Cr intermetallic compounds are the main inclusions in this diamond sample and are exposed on chip surfaces as separate micron-sized particles and aggregates in the form of chains 20 μm long. In some places, they form dendritic aggregates of the same size. The ED spectra exhibit Fe and Cr peaks, the former being higher than the latter. According to the semiquantitative analysis, the Cr content in the intermetallic compounds varies from 12.8 to 13.2 wt %.

Pentlandite [$(Fe, Ni)_9S_8$]. Several particles of Fe–Ni sulfide were revealed on the surfaces of chips of diamond crystal 2. They are devoid of crystallographic forms and do not exceed 1 μm in size (Fig. 3e). The ED spectra demonstrate Fe, Ni, and S peaks (Fig. 3f). According to the semiquantitative analysis, their formula fits pentlandite [$(Fe, Ni)_9S_8$].

Garnet. One microcrystal about 5 μm across was revealed. It corresponds to pyrope–andradite in composition, i.e., belongs to the eclogite assemblage of inclusions in diamonds.

Crystal 3

Native iron (α-Fe) is represented in the sample by several particles measuring fractions of a micron in size and their aggregates. The ED spectra of these segregations reveal only Fe peaks.

Fe–Cr intermetallic compounds are represented by many discrete rounded and tear-shaped particles. Their size does not exceed 0.5 μm. The ED spectra contain only Fe and Cr peaks (Fe ⩾ Cr). According to the semiquantitative analysis, the Cr content varies from 11.5 to 12 wt %.

Apatite was revealed as a single elongated microcrystal about 10 × 15 μm in size. Fluorine was detected in its composition in addition to Ca, P, and O; thus, the mineral belongs to fluorapatite.

An aggregate of diopside [$(Ca, Mg)Si_2O_6$], calcite, and apatite [$Ca_5(PO_4)_3OH$] makes up a large inclusion of irregularly curved shape about 270 μm long and 80–100 μm wide related to rather a large mechanical fracture that initially cut this crystal (Fig. 4a). The bulk of this inclusion consists of clinopyroxene, the composition of which at most analyzed points is close to diopside [$(Ca, Mg)Si_2O_6$] (Fig. 4b). In one portion of this silicate, fine-grained segregations somewhat brighter than diopside were detected in the BSE image (Fig. 4c). The ED spectrum of these segregations (Fig. 4d) contains main Ca, C, and O peaks. The results of the semiquantitative analysis indicate that this mineral is calcite ($CaCO_3$).

On another part of the diopside surface, bright isometric and sharp-cornered areas with dimensions of 5–30 μm were exposed (Fig. 4e). In composition, this mineral corresponds to apatite (Fig. 4f) containing about 4 wt % F and 1 wt % Sr.

Crystal 4

A porous texture typical of polycrystalline diamond aggregates is observed on the surfaces of some chips of this diamond. Pores vary from 3 to 5 μm in size.

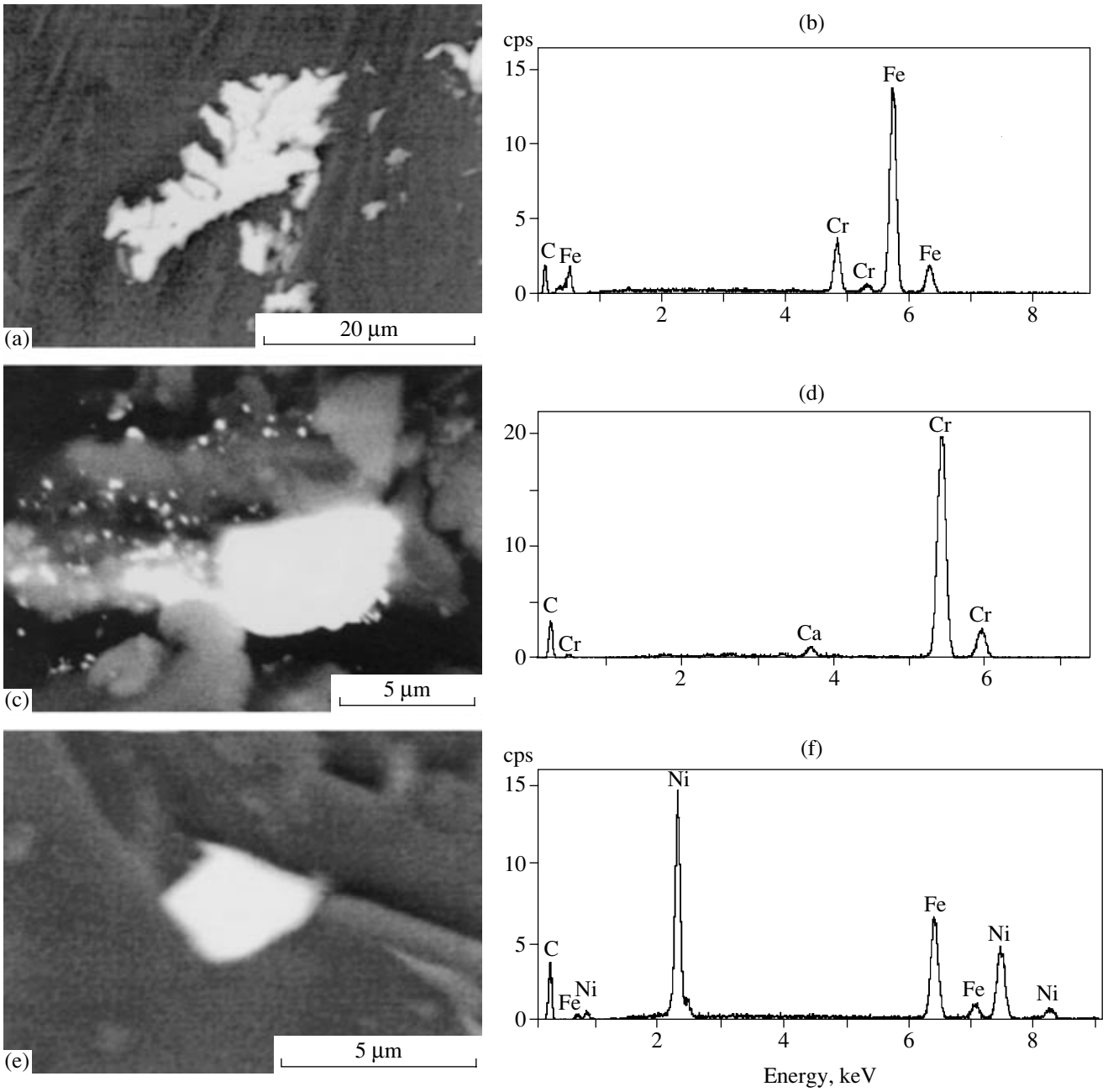

Fig. 3. BSE images and ED spectra of microinclusions on the surfaces of chips of diamond crystals. (a, b) Fe–Cr intermetallic compounds; (c, d) native chrome; (e, f) pentlandite.

Locally, the chip surface exhibits a microblock structure.

Fe–Cr intermetallic compounds are the main inclusions in this sample. Clusters of their particles and aggregates were revealed on the chip surfaces, with their size varying from fractions of a micrometer to 10 μm. The ED spectra of different particles contain Fe and Cr peaks (Fe ⩾ Cr). The Cr content varies from 1.0 to 13.7 wt %.

Native iron (α-Fe) is detected on the chip surfaces less frequently than the Fe–Cr intermetallic compounds. Native iron is detected as both separate grains and aggregates. The size of discrete particles reaches 1 μm. According to the semiquantitative analysis, the bulk of α-Fe contains no impurities.

Calcite. Aggregates of this mineral form irregular segregations in some parts of the sample; their size varies from 5 to 10 μm.

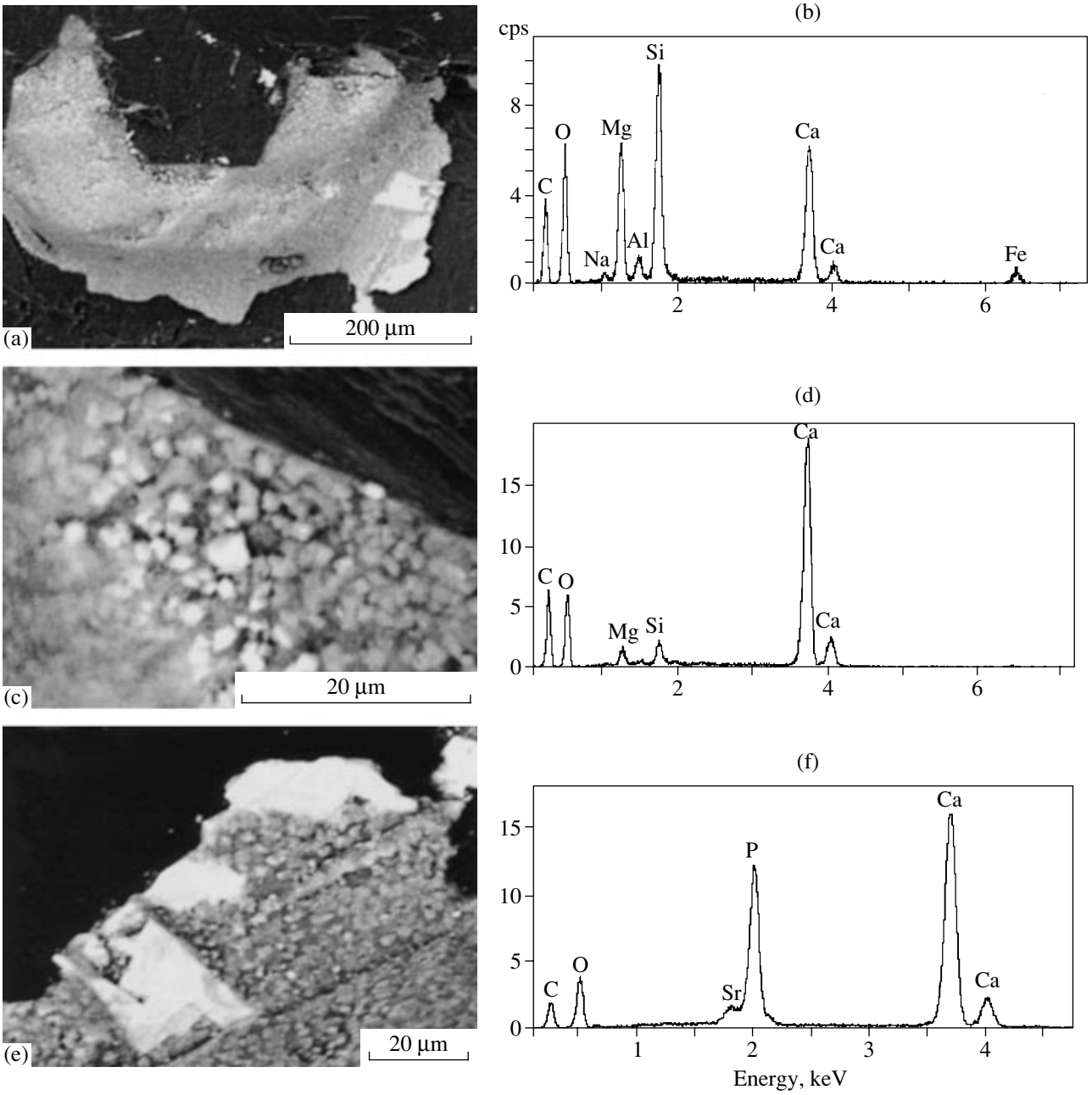

Fig. 4. BSE images and ED spectra of a microinclusion representing an intergrowth of clinopyroxene, calcite, and apatite on the surface of a chip of diamond crystal 3. (a, b) Clinopyroxene of the inclusion bulk; (c, d) calcite; (e, f) apatite.

DISCUSSION

The scanning electron microscopy results show that rather perfect transparent diamond crystals of octahedral habit from the China kimberlites generally contain a relatively small amount of microinclusions as compared with previously studied opaque diamond crystals of cubic habit (Gorshkov et al., 1997b; Vinokurov et al., 1998) and polycrystalline aggregates (bort) (Gorshkov et al., 2000) from the same deposits.

The occurrence of native metals as inclusions is a common feature of octahedral crystals and the previously studied crystals of cubic habit and polycrystalline diamond aggregates from the China kimberlites. Native iron and Fe–Cr intermetallic compounds, which are exposed on the surface of samples and occur within them, are the most abundant. Inclusions of native chrome and lead, as well as native tungsten, identified for the first time, were also revealed on the surface of crystals.

It should be noted that inclusions of native iron and silver, as well as Fe–Au intermetallic compounds with a Ag admixture, were previously reported from dia-

mond crystals incorporated into the China kimberlites (Zhao, 1995).

The studied crystals are similar in respect to native metal microinclusions to most imperfect semitransparent diamonds studied previously at different deposits of the world using analytical electron microscopy. Microinclusions of native metals were detected in polycrystalline aggregates from the Yakutian deposits, in polycrystalline aggregates (carbonado) from placer deposits of Brazil and central Africa, in rounded crystals from lamproites of Australia, in shapeless dark diamonds from impactites of the Popigai ring structure, and in samples from other sources (Gorshkov et al., 2003; Titkov et al., 2003, 2004). Relatively large inclusions of native metals in diamonds from the Yakutian deposits were revealed using standard microprobe analysis (Sobolev et al., 1981; Bulanova et al., 1998).

One microcrystal of Cr-free garnet and a large aggregate of clinopyroxene heterogeneous in composition were established in the studied samples. These minerals belong to the eclogite assemblage of inclusions in diamonds, although a considerable prevalence of inclusions of the peridotite assemblage was previously established in diamonds from the China kimberlites (Harris et al., 1994; Meyer et al., 1994). Clinopyroxene heterogeneous in composition forms close intergrowths with calcite and apatite. Intergrowths of $CaCO_3$ and $MgCO_3$ phases with clino- and orthopyroxene aggregates as inclusions in diamonds were previously reported from placer deposits of Namibia (Leost et al., 2003). Intergrowths of $CaCO_3$ phase with olivine (McDade and Harris, 1999) and with phlogopite (Sobolev et al., 1997) were also noted. Enstatite–calcite intergrowths in diamonds have been observed in imperfect diamond crystals from the Yakutian deposits; the results of their investigation will be considered in a forthcoming paper.

The intergrowths of silicates with carbonates as inclusions in diamonds have important genetic implications. As has been experimentally established recently, diamonds may crystallize directly from carbonate and carbonate–silicate melts (Akaishi et al., 1990), as well as during interaction of carbonates and silicates (Pal'yanov et al., 2002). The data on carbonate–silicate inclusions indicate that similar processes probably took place during the formation of natural diamonds as well. The intergrowths of clinopyroxene and apatite show that phosphorus was involved in this process.

The dendritelike sylvite structures established on the surface of one of the samples and discrete matlockite particles hardly are random findings. Inclusions of chlorides (sylvite and halite) were observed previously in very imperfect diamonds: in a crystal of cubic habit from the China kimberlites (Vinokurov et al., 1998), in rounded crystals from lamproites of Australia (Gorshkov et al., 2003), and in coarse-grained aggregates from the Yakutian kimberlites (Titkov et al., 2003). Fluid inclusions containing carbonates, Cl, K, Na, and other elements that were found in central parts of perfect diamond crystals from the South African kimberlites (Izraeli et al., 2003) indicate that chloride inclusions are genetically related to diamond crystallization and did not form in the course of epigenetic processes. As was mentioned above, one possible explanation for the formation of unusual associations of inclusions in natural diamonds is their crystallization during injection of fluids into deep-seated rocks (Taylor and Green, 1988). Metasomatism of deep-seated rocks and formation of carbonate–silicate melts and chloride–carbonate brines might have taken place in the course of this complicated dynamic process (Izraeli et al., 2003). The fluids were probably a source of native metals, inclusions of which are detected in natural diamonds. It should be pointed out in this connection that a mantle origin was also established for chlorides and carbonates of alkaline metals from slightly altered kimberlites of the Udachnaya–Vostochnaya pipe (Kamenetsky et al., 2004).

ACKNOWLEDGMENTS

This study was supported by the Russian Foundation for Basic Research, project no. 04-05-64606.

REFERENCES

1. M. Akaishi, H. Kanda, and S. Yamaoka. "Synthesis of Diamond from Graphite-Carbonate Systems under Very High Temperature and Pressure," J. Crystal Growth **104**, 578–581 (1990).
2. G. P. Bulanova, W. L. Griffin, and C. G. Ryan, "Nucleation Environment of Diamonds from Yakutian Kimberlites," Mineral. Mag. **62** (3), 409–419 (1998).
3. A. I. Gorshkov, Y. N. Bao, L. V. Bershov, et al., Inclusions in Diamond from the Liaoning Deposit (China) and Their Genetic Implications, Geokhimiya **35** (1), 58–65 (1997a) [Geochem. Intern. **35** (1), 51–57 (1997a)].
4. A. I. Gorshkov, Y. N. Bao, L. V. Bershov, et al., "Inclusions of Native Metals and Other Minerals in Diamond from Kimberlite Pipe 50, Liaoning, China," Geokhimiya **35** (1), 58–65 (1997b) [Geochem. Int. **35** (1), 965–703 (1997b)].
5. A. I. Gorshkov, Y. N. Bao, S. V. Titkov, et al., "Polycrystalline Diamond Aggregate (Bort) from the Shengli Kimberlite Pipe, China: Growth Features, Mineral Inclusions, and Genesis," Geokhimiya **37** (1), 82–89 (1999) [Geochem. Intern. **37** (1), 75–81 (1999)].
6. A. I. Gorshkov, Y. N. Bao, S. V. Titkov, et al., "Composition of Mineral Inclusions and Formation of Polycrystalline Diamond Aggregates (Bort) from the Shengli Kimberlite Pipe," Geokhimiya **38** (7), 769–776 (2000) [Geochem. Intern. **38** (7), 698–705 (2000)].
7. A. I. Gorshkov, L. V. Bershov, S. V. Titkov, et al., "Composition of Mineral Inclusions and Admixtures in Diamond from Lamproites of Argyle Kimberlite Pipe (Western Australia)," Geokhimiya **41** (12), 1251–1261 (2003) [Geochem. Intern. **41** (12), (2003)].
8. J. W. Harris, D. J. Duncan, F. Zhang, et al., "The Physical Characteristics and Syngenetic Inclusions Geochemistry

of Diamonds from Pipe 50, Liaoning Province, People's Republic of China," in *Proceedings of the 5th Intern. Kimberlite Conference* (Araxa, 1994), pp. 106–115.

9. E. Izraeli, J. W. Harris, and O. Navon, "Fluid in Mineral Inclusions in Cloudy Diamonds from Koffifontein, South Africa," Geochim. Cosmochim. Acta **68**, 2561–2575 (2003).
10. M. B. Kamenetsky, A. V. Sobolev, V. S. Kamenetsky, et al., "Kimberlite Melts Rich in Alkali Chlorides and Carbonates: A Potent Metasomatic Agent in the Mantle," Geology **32** (10), 2561–2575 (2004).
11. I. Leost, T. Stachel, G. Brey, et al., "Diamond Formation and Source Carbonation: Mineral Associations in Diamonds from Namibia," Contrib. Mineral. Petrol. **145**, 15–24 (2003).
12. J. S. Leung, "Silicon Carbide Cluster Entrapped in a Diamond from Fuxon, Ghana," Am. Mineral. **75** (9–10), 1110–1119 (1990).
13. P. McDade and J. W. Harris, "Syngenetic Inclusion Bearing Diamonds from the Letseng-la-Terai, Lesotho," in *Proceedings of the 7th Intern. Kimberlite Conference* (Capetown, 1999), Vol. 2, pp. 557–565.
14. H. O. A. Meyer, A. Zhang, H. J. Milledge, and M. J. Mendelssohn, "Diamonds and Inclusions in Diamonds from Chinese Kimberlites," in *Proceedings of the 5th International kimberlite Conference* (Araxa, 1994), pp. 98–105.
15. Y. N. Pal'yanov, A. G. Sokol, Y. M. Borzdov, et al., "Diamond Formation through Carbonate-Silicate Interaction," Am. Mineral. **87** (7), 1009–1013 (2002).
16. E. I. Semenov and E. P. Zarubeeva, *Glossary of Mineralogy* (Fersman Mineral. Museum, Moscow, 1998) [in Russian].
17. N. V. Sobolev, E. S. Efimova, and L. N. Pospelova, "Native Iron in Diamonds of Yakutia and Its Paragenesis," Geol. Geofiz. **22** (12), 25–28 (1981).
18. N. V. Sobolev, F. V. Kaminsky, W. L. Griffin, et al., "Mineral Inclusions in Diamonds from the Sputnic Kimberlite Pipe, Yakutia Source," Lithos **39**, 135–157 (1997).
19. W. R. Taylor and D. H. Green, "The Role of Reduced C–O–H Fluids in Mantle Partial Melting," in *Kimberlites and Related Rocks* (Geol. Soc. Australia Spec. Publ., 1988), Vol. 1, No. 14, pp. 592–602.
20. S. V. Titkov, A. I. Gorshkov, L. O. Magazina, et al., "Shapeless Dark Diamonds (Yakutites) from Placers at the Siberia Craton and Criteria of Their Impact Genesis," Geol. Rudn. Mestorozhd. **46** (3), 222–234 (2004) [Geol. Ore Deposits **46** (3), 191–201 (2004)].
21. S. V. Titkov, N. G. Zudin, A. I. Gorshkov, et al., "An Investigation into the Cause of Colour in Natural Black Diamonds from Siberia," Gems and Gemology **39** (3), 200–209 (2003).
22. S. F. Vinokurov, A. I. Gorshkov, Yan Nan Bao, et al., "Diamonds from Kimberlite Diatreme 50, Liaoning Province, China: Microtextural, Mineralogical, Geochemical, and Genetic Characteristics," Geokhimiya **36** (8), 759–767 (1998) [Geochem. Int. **36** (8), 676–683 (1998)].
23. L. Zhao, "The First Discovery of Native Silver and Silver-Bearing Fe–Au Alloy Inclusions in Diamonds," Chinese Sci. Bull. **40** (12), 1114–1115 (1995).